

Deterministic generation of multi-photon bundles in a quantum Rabi model

Cheng Liu,¹ Jin-Feng Huang,^{1,*} and Lin Tian²

¹*Key Laboratory of Low-Dimensional Quantum Structures and Quantum Control of Ministry of Education, Key Laboratory for Matter Microstructure and Function of Hunan Province, Department of Physics and Synergetic Innovation Center for Quantum Effects and Applications, Hunan Normal University, Changsha 410081, China*

²*School of Natural Sciences, University of California, Merced, California 95343, USA*

(Dated: October 10, 2022)

Multi-photon bundle states are crucial for a broad range of applications such as quantum metrology, quantum lithography, quantum communications, and quantum biology. Here we propose a scheme that generates multi-photon bundles via virtual excitations in a quantum Rabi model. Our approach utilizes a Ξ -type three-level atom, where the upper two levels are coupled to a cavity field to form a quantum Rabi model with ultrastrong coupling strength, and the transition between the lower two levels is driven by two sequences of Gaussian pulses. We show that the driving pulses induce the emission of virtual photons from the ground state of the quantum Rabi model via the stimulated Raman adiabatic passage technique, and hence can create bundles of even-numbered photons deterministically and dynamically in the cavity output field. We also study the generalized second-order correlation functions of the output photons, which reveal that the generated photons form an antibunched multi-photon emitter.

I. INTRODUCTION

Light-atom interaction plays a key role in quantum optics and quantum information. The quantum Rabi model (QRM), which describes the interaction of a bosonic mode with a two-level atom, is essential in quantum optics and quantum science. With the progress in experimental technology in the last few decades, the light-atom interaction strength can now exceed 10% of the light frequency or the atomic transition frequency [1–6], which is denoted as the ultrastrong coupling regime, or can even be comparable to the light or atomic frequencies, which is called the deep-strong coupling regime [7–9]. The ultrastrong coupling regime can be implemented with various systems including the superconducting quantum devices [1, 2, 7, 9], intersubband polaritons [5], Landau polaritons [8, 10], organic molecules [3, 6], and optomechanical systems [4]. Many interesting phenomena resulted from the ultrastrong or deep-strong coupling have been studied or demonstrated in these systems, such as vacuum degeneracy [11], photon blockade [12], few-photon scattering [13, 14], quantum phase transition [15–17], multi-photon Rabi oscillation [18, 19], manipulating counter-rotating interaction [20–23], and few-photon emission [24–26]. Due to the ultrastrong coupling, the rotating-wave approximation (RWA) fails, and the ground state of the QRM carries virtual photons that cannot be detected and used directly. Some schemes such as spontaneous emission [24], stimulated emission [25], and electroluminescence [26] have been proposed to generate real photons by converting the virtual photons in the ground state of the QRM.

Recently, multi-quanta physics has attracted enormous interest because of its potential applications. In particular, the emission of multi-photon bundles [27] has important applications in the generation of new light source [28, 29], quantum metrology [30, 31], quantum lithography [32], quantum

communications [33], quantum biology [34, 35], and medical applications [36, 37]. The multi-photon bundle emission can be defined as multiple photons being emitted in a bundle that is antibunched. People have investigated the generation of multi-photon bundles in various setups, such as Rydberg atomic ensembles [38, 39], Kerr cavity systems [40, 41], multi-level atomic systems [42–45], cavity quantum electrodynamics (QED) systems [27, 46–49], superconducting circuits [50], and waveguide-QED systems [51–53]. However, because the high-order processes of single-photon transition are weak, multi-photon bundle emission is challenging to achieve experimentally.

Here, we propose an efficient scheme to generate multi-photon bundles via the stimulated Raman adiabatic passage (STIRAP) technique [54–56], where the multiple virtual photons of the ground state of a QRM are emitted as cavity photons, and subsequently released from the cavity in a bundle. In this scheme, the multi-photon bundle is emitted on demand, controlled by external driving pulses. To be specific, we study a Ξ -type atom with the upper two levels of the atom coupled to a cavity field with ultrastrong coupling, while the transition between the lower two levels of the atom is driven by two sequences of external Gaussian pulses. By choosing appropriate resonance conditions, we can create a Λ -type three-level system, where one of the lower level contains even number of cavity photons. By applying the STIRAP technique, the system can be deterministically prepared to the lower level with cavity photons, which will be emitted as multi-photon bundle via cavity dissipation. Using the quantum trajectory technique, we demonstrate the dynamical emission of multi-photon bundles from the cavity. We also calculate the standard and generalized second-order correlation functions, which shows the antibunching nature of the emitted multi-photon bundles. Our scheme connects virtual photons in the QRM with on-demand, efficient multi-photon bundle emission, and provides a new mechanism for the deterministic generation of multi-photon sources.

* Corresponding author: jfhuang@hunnu.edu.cn

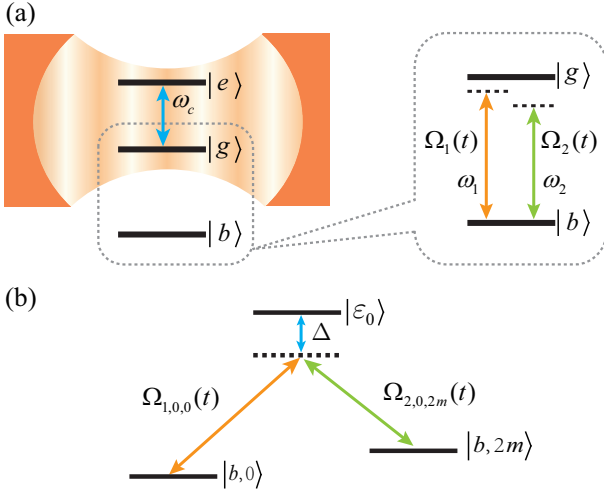


FIG. 1. (Color online) (a) Schematic of the system with a Ξ -type three-level atom coupled to a cavity mode through the upper two levels $|e\rangle$ and $|g\rangle$. The transition between the lower two levels $|g\rangle$ and $|b\rangle$ is driven by two external driving fields with driving frequency ω_l ($l = 1, 2$) and time-dependent driving amplitude $\Omega_l(t)$. (b) Energy structure of the effective Λ -type three-level system. The initial state $|b, 0\rangle$ and the final state $|b, 2m\rangle$ are coupled by the drive fields with the effective coupling strengths $\Omega_{1,0,0}(t)$ and $\Omega_{2,0,2m}(t)$ via the ground state $|\varepsilon_0\rangle$ of the quantum Rabi model. The detuning Δ is the difference between the driving frequency ω_1 (ω_2) and the transition frequency from $|b, 0\rangle$ ($|b, 2m\rangle$) to $|\varepsilon_0\rangle$.

II. MODEL

We consider a Ξ -type three-level atom where the upper two levels $|e\rangle$ and $|g\rangle$ are coupled to a cavity mode with ultrastrong coupling, the transition between the lower two levels $|g\rangle$ and $|b\rangle$ is driven by two external driving fields with driving frequency ω_l ($l = 1, 2$) and composed of consecutive Gaussian wave packets. The frequency difference between the lower levels $|g\rangle - |b\rangle$ is much greater than both the cavity frequency ω_c and the frequency difference between the upper levels $|e\rangle - |g\rangle$ so that the bottom level $|b\rangle$ is not coupled to the cavity mode and the driving fields do not induce transition between the upper levels, as shown in Fig. 1(a). The system Hamiltonian can be written as ($\hbar = 1$)

$$H(t) = \sum_{s=e,g,b} \omega_s |s\rangle \langle s| + \omega_c a^\dagger a + \lambda(a + a^\dagger)(|e\rangle \langle g| + |g\rangle \langle e|) + \sum_{l=1}^2 [\Omega_l(t) \cos(\omega_l t)] (|b\rangle \langle g| + |g\rangle \langle b|) \quad (1)$$

with time-dependent driving amplitude

$$\Omega_l(t) = \Omega_l \sum_{k=0}^{\infty} \exp\left[-\frac{(t - t_l - kT_1)^2}{T^2}\right], \quad (l = 1, 2). \quad (2)$$

Here, a (a^\dagger) is the annihilation (creation) operator of the cavity mode with resonance frequency ω_c , ω_s is the frequency for the energy level $|s\rangle$ ($s = e, g, b$), and λ is the atom-cavity

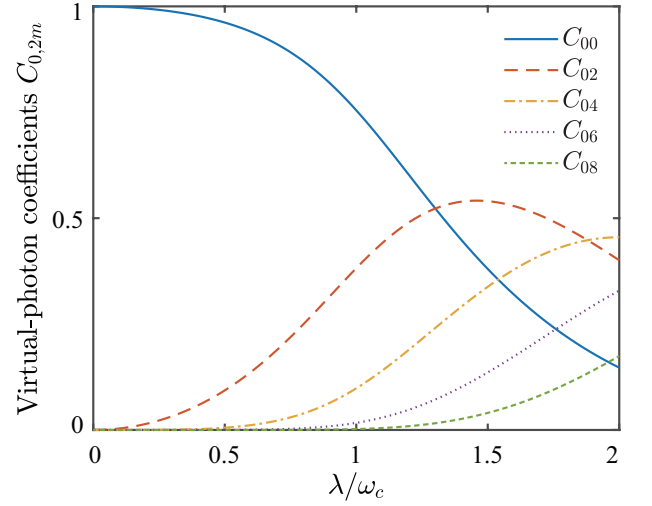


FIG. 2. (Color online) Coefficient $C_{0,2m}$ of $|g, 2m\rangle$ ($m = 0, 1, \dots, 4$) in the ground state $|\varepsilon_0\rangle$ of H_R as a function of the ratio λ/ω_c for the resonant case $\omega_c = \omega_e - \omega_g$.

coupling strength. The parameters Ω_l and T denote the maximum amplitude and the width of the Gaussian pulses, respectively, and t_l ($l = 1, 2$) is the time of the maximum value of the first Gaussian pulse wave packet, k is an integer labelling the pulses in the driving field, and T_1 is the time interval between consecutive Gaussian pulses.

The Hamiltonian of the upper two levels and the cavity mode $H_R = \omega_e |e\rangle \langle e| + \omega_g |g\rangle \langle g| + \omega_c a^\dagger a (|e\rangle \langle e| + |g\rangle \langle g|) + \lambda(a + a^\dagger)(|e\rangle \langle g| + |g\rangle \langle e|)$ within the total Hamiltonian $H(t)$ is exactly the quantum Rabi Hamiltonian [57]. The total Hamiltonian $H(t)$ can hence be written as $H(t) = H_R + \omega_b |b\rangle \langle b| + \omega_c a^\dagger a |b\rangle \langle b| + \sum_{l=1}^2 [\Omega_l(t) \cos(\omega_l t)] (|b\rangle \langle g| + |g\rangle \langle b|)$. In terms of the eigenstate $|\varepsilon_n\rangle$ of H_R , the first three terms in Eq. (1) can then be written in the diagonal form:

$$H_0 = \sum_{n=0}^{\infty} [\varepsilon_n |\varepsilon_n\rangle \langle \varepsilon_n| + (\omega_b + n\omega_c) |b, n\rangle \langle b, n|]. \quad (3)$$

The eigenstate $|\varepsilon_n\rangle$ can be expressed as $|\varepsilon_n\rangle = \sum_{m=0}^{\infty} (C_{n,m} |g, m\rangle + D_{n,m} |e, m\rangle)$ in terms of the uncoupled atomic and cavity states with real probability amplitudes $C_{n,m} = \langle \varepsilon_n | g, m \rangle$ and $D_{n,m} = \langle \varepsilon_n | e, m \rangle$, which can be numerically obtained. Meanwhile, in terms of the eigenstate $|\varepsilon_n\rangle$, the last term in Eq. (1) can be written as

$$H_D(t) = \sum_{n,m=0}^{\infty} \sum_{l=1}^2 [\Omega_l(t) \cos(\omega_l t)] C_{n,m} |\varepsilon_n\rangle \langle b, m| + \text{H.c.} \quad (4)$$

In the rotating frame defined by the unitary operator $U(t) = \exp(-iH_0 t)$, the system Hamiltonian becomes

$$H_I(t) = \sum_{n,m=0}^{\infty} \sum_{l=1}^2 \sum_{p=\pm 1} [\Omega_{l,n,m}(t) e^{i\Delta_{n,m,p,t}}] |\varepsilon_n\rangle \langle b, m| + \text{H.c.}, \quad (5)$$

where the effective coupling strength $\Omega_{l,n,m}(t)$ and the detun-

ing $\Delta_{n,m,p,l}$ are respectively defined as

$$\begin{aligned}\Omega_{l,n,m}(t) &= \frac{C_{n,m}}{2} \Omega_l(t), \quad (l = 1, 2), \\ \Delta_{n,m,p,l} &= \varepsilon_n - \omega_b - m\omega_c + p\omega_l.\end{aligned}\quad (6)$$

Here the effective coupling strength is modified by the probability amplitudes $C_{n,m}$ ($n, m \geq 0$ being integer). It is worth noting that the total number of excitations in the QRM is not a conserved quantity due to the existence of the counter-rotating terms, but the QRM possesses a parity (or \mathbb{Z}_2) symmetry which shows that the system is integrable [58]. It can be shown that the ground state of H_R only contains states with even number of excitations, and can be expanded as $|\varepsilon_0\rangle = \sum_{m=0}^{\infty} (C_{0,2m}|g, 2m\rangle + D_{0,2m+1}|e, 2m+1\rangle)$. Hence in the ground state, the amplitudes of states with odd number of photons and the atom being in the state $|g\rangle$ satisfy $C_{0,2m+1} = 0$ due the parity symmetry [58]. The photons in the state $|\varepsilon_0\rangle$ are bounded (or virtual), and cannot be detected directly. To see clearly the dependence of the virtual photon amplitudes on the coupling strength λ , we plot the coefficients $C_{0,2m}$ ($m = 0, 1, \dots, 4$) as a function of the ratio λ/ω_c in Fig. 2. When the coupling strength λ/ω_c is small, i.e., $\lambda/\omega_c \ll 0.1$, the Hamiltonian H_R is reduced to the Jaynes-Cummings (JC) Hamiltonian under the RWA. In this regime, we can find that the ground state $|\varepsilon_0\rangle$ is mainly composed of $|g, 0\rangle$ with zero excitation. In this regime, the population transfer from the states $|b, 0\rangle$ to $|b, 2m\rangle$ ($m > 0$) will not occur due to the small amplitudes of the states $|g, 2m\rangle$ ($m > 0$). Therefore, in order to generate multiple photons, the atom-cavity coupling is required to be in the either ultrastrong or deep-strong coupling regime, where $C_{0,2m}$ ($m > 0$) will become significant.

III. STIRAP GENERATION OF MULTIPLE PHOTONS

In this section, we derive an effective Hamiltonian of the above system under the $2m$ -photon (m being positive integer) resonance condition [25]

$$\omega_1 - \omega_2 = 2m\omega_c, \quad (7)$$

and elucidate the physical mechanism of coherent population transfer from the initial state $|b, 0\rangle$ to the final state $|b, 2m\rangle$ based on the STIRAP technique. We will then discuss the generation of 2 and 4 photons in detail.

A. Effective Hamiltonian and photon generation

Assume that the system is in the initial state $|b, 0\rangle$ with the cavity field in vacuum and the atom in the lowest state $|b\rangle$. Let the driving frequencies be near resonance with both the transition frequency $\varepsilon_0 - \omega_b$ and the $2m$ -photon emission frequency $\varepsilon_0 - \omega_b - 2m\omega_c$, respectively, i.e., $\Delta_{0,0,-1,1}, \Delta_{0,2m,-1,2} \ll 2m\omega_c$, and the excited states $|\varepsilon_n\rangle$ ($n > 0$) are far detuned from the driving frequencies so that they can be neglected from this scheme. Under the $2m$ -photon resonance condition (7), the

Hamiltonian (5) can be reduced to

$$\begin{aligned}\tilde{H}_I(t) &= \Omega_{1,0,0}(t) e^{i\Delta_{0,0,-1,1}t} |\varepsilon_0\rangle \langle b, 0| \\ &+ \Omega_{2,0,2m}(t) e^{i\Delta_{0,2m,-1,2}t} |\varepsilon_0\rangle \langle b, 2m| + \text{H.c.},\end{aligned}\quad (8)$$

which only connects the states with even number of photons $|b, 2m\rangle$ to the ground state $|\varepsilon_0\rangle$ of the QRM as $C_{0,2m+1} = 0$ ($m = 0, 1, \dots$). Here we have ignored the fast oscillating terms under the RWA by the condition $|\Omega_{l,n,m}(t)/\Delta_{n,m,+1,l}| \ll 1$ and $|\Omega_{l,n,m}(t)/\Delta_{n,m,-1,l}| \ll 1$ ($n \geq 1, l = 1, 2$). The system can then be reduced to an effective three-level system, as shown in Fig. 1(b).

With the $2m$ -photon resonance condition (7), $\Delta_{0,0,-1,1} = \Delta_{0,2m,-1,2} \equiv \Delta$. In a rotating frame with respect to $\tilde{H}_0 = -\Delta|\varepsilon_0\rangle\langle\varepsilon_0|$, we obtain the effective Hamiltonian for this system:

$$\begin{aligned}H_{\text{eff}}^{(2m)} &= \Delta|\varepsilon_0\rangle\langle\varepsilon_0| + [\Omega_{1,0,0}(t)|\varepsilon_0\rangle\langle b, 0| \\ &+ \Omega_{2,0,2m}(t)|\varepsilon_0\rangle\langle b, 2m| + \text{H.c.}].\end{aligned}\quad (9)$$

This Hamiltonian describes a Λ -type three-level system, where the effective coupling strength $\Omega_{1,0,0}(t)$ [$\Omega_{2,0,2m}(t)$] depends on the virtual-photon coefficient $C_{0,0}$ ($C_{0,2m}$). The coupling strength $\Omega_{1,0,0}(t)$ [$\Omega_{2,0,2m}(t)$] can be tuned by choosing appropriate coupling strength λ , which can strongly affect the coefficients $C_{0,0}$ and $C_{0,2m}$ according to Fig. 2. The transfer from the state $|b, 0\rangle$ with the cavity in the vacuum state to the state $|b, 2m\rangle$ with $2m$ cavity photons can be achieved through these two couplings, which is the key mechanism for our scheme to generate multiple photons.

In our scheme, the coupling strengths $\Omega_{1,0,0}(t)$ and $\Omega_{2,0,2m}(t)$ in Eq. (9) are time dependent. We derive the instantaneous eigenstates of the effective Hamiltonian (9) at time t as follows

$$|\psi_0^{(2m)}(t)\rangle = \cos\theta_{2m}(t)|b, 0\rangle - \sin\theta_{2m}(t)|b, 2m\rangle, \quad (10a)$$

$$\begin{aligned}|\psi_+^{(2m)}(t)\rangle &= \sin\varphi_{2m}(t)[\sin\theta_{2m}(t)|b, 0\rangle + \cos\theta_{2m}(t)|b, 2m\rangle] \\ &+ \cos\varphi_{2m}(t)|\varepsilon_0\rangle,\end{aligned}\quad (10b)$$

$$\begin{aligned}|\psi_-^{(2m)}(t)\rangle &= \cos\varphi_{2m}(t)[\sin\theta_{2m}(t)|b, 0\rangle + \cos\theta_{2m}(t)|b, 2m\rangle] \\ &- \sin\varphi_{2m}(t)|\varepsilon_0\rangle,\end{aligned}\quad (10c)$$

and the corresponding instantaneous eigenvalues are $\lambda_0 = 0$, $\lambda_+ = \tilde{\Omega}_{2m}(t) \cot\varphi_{2m}(t)$, and $\lambda_- = -\tilde{\Omega}_{2m}(t) \tan\varphi_{2m}(t)$, where

$$\theta_{2m}(t) = \arctan\left[\frac{\eta_{2m}\Omega_1(t)}{\Omega_2(t)}\right], \quad (11a)$$

$$\varphi_{2m}(t) = \arctan\left[\frac{\tilde{\Omega}_{2m}(t)}{\frac{\Delta}{2} + \sqrt{\frac{\Delta^2}{4} + \tilde{\Omega}_{2m}^2(t)}}\right], \quad (11b)$$

with

$$\tilde{\Omega}_{2m}(t) = \frac{|C_{0,2m}|}{2} \sqrt{\eta_{2m}^2 \Omega_1^2(t) + \Omega_2^2(t)} \quad (12)$$

and $\eta_{2m} = |C_{0,0}/C_{0,2m}|$. The eigenstate $|\psi_0^{(2m)}(t)\rangle$ in Eq. (10a) with eigenvalue $\lambda_0 = 0$ is a dark state, which does not include

the state $|\varepsilon_0\rangle$ as its component. Instead, the dark state is a coherent superposition of the vacuum state and the $2m$ -photon state of the cavity with the atom in the lowest level $|b\rangle$. With the system initially prepared in the dark state $|\psi_0^{(2m)}(t)\rangle$ and the effective coupling strengths tuned adiabatically under the condition [54–56]: $|\dot{\theta}_{2m}(t)| \ll |\lambda_{\pm} - \lambda_0|$, which leads to

$$|\dot{\theta}_{2m}(t)| \ll \left| \frac{\Delta}{2} \pm \sqrt{\frac{\Delta^2}{4} + \tilde{\Omega}_{2m}^2(t)} \right|, \quad (13)$$

the system will remain in the dark state $|\psi_0^{(2m)}(t)\rangle$ at an arbitrary time t during the evolution. Thus, by adjusting the driving amplitudes appropriately, the system state can be converted from an initial dark state to a desired dark state at the end of the evolution using the STIRAP technique. In our approach, the initial state at $t = 0$ is prepared in the dark state $|\psi_0^{(2m)}(0)\rangle = |b, 0\rangle$ for $\theta_{2m} = 0$, and at the final time t , $\theta_{2m} = \pi/2$, which corresponds to the dark state $|b, 2m\rangle$. By increasing θ_{2m} adiabatically under the condition (13), we can hence convert the state $|b, 0\rangle$ to the multi-photon state $|b, 2m\rangle$. The merit of the STIRAP technique is that it only involves the dark state (not the state $|\varepsilon_0\rangle$), which will not decay to the lowest atomic level $|b\rangle$ via spontaneous emission. Moreover, as $|b\rangle$ is not coupled to the cavity mode, the photons are emitted only through the STIRAP process. The process is thus fully deterministic via external control fields.

In the following, we will discuss the generation of two and four photons in detail for the detuning $\Delta = 0$.

B. Two-photon generation

We first choose $m=1$ in the Hamiltonian (9) for the generation of two photons, which requires $\omega_1 - \omega_2 = 2\omega_c$. At $\Delta = 0$, the effective Hamiltonian (9) becomes

$$H_{\text{eff}}^{(2)}(t) = \Omega_{1,0,0}(t) |\varepsilon_0\rangle \langle b, 0| + \Omega_{2,0,2}(t) |\varepsilon_0\rangle \langle b, 2| + \text{H.c.}, \quad (14)$$

and the corresponding dark state (10a) becomes

$$|\psi_0^{(2)}(t)\rangle = \cos \theta_2(t) |b, 0\rangle - \sin \theta_2(t) |b, 2m\rangle \quad (15)$$

with angle $\theta_2(t) = \arctan[\eta_2^2 \Omega_1(t) / \Omega_2(t)]$.

To generate two photons with STIRAP, the system is required to adiabatically follow the dark state $|\psi_0^{(2)}(t)\rangle$ during the evolution [54, 55]. Let the initial state at time $t = 0$ be the dark state $|\psi_0^{(2)}(t)\rangle = |b, 0\rangle$ for $\theta_2(t) = 0$, which requires $\Omega_1(t) / \Omega_2(t) \rightarrow 0$. We then adiabatically change $\theta_2(t)$ to reach $\theta_2(t) = \pi/2$, which corresponds to $\Omega_1(t) / \Omega_2(t) \rightarrow \infty$. At time t , the dark state is $|\psi_0^{(2)}(t)\rangle = |b, 2\rangle$, which is the atomic state $|b\rangle$ plus two cavity photons. Note that the efficient implementation of the STIRAP process requires that the two pulses $\Omega_1(t)$ and $\Omega_2(t)$ have significant overlap in time, as shown in Fig. 3(a). The effective coupling strengths $\Omega_{1,0,0}(t)$ and $\Omega_{2,0,2}(t)$ are plotted in Fig. 3(b), where the maximum values of the two couplings are equal to each other. It is worth mentioning that the pulse $\Omega_2(t)$ is applied before $\Omega_1(t)$, which is counter-intuitive but typical in STIRAP. To demonstrate the

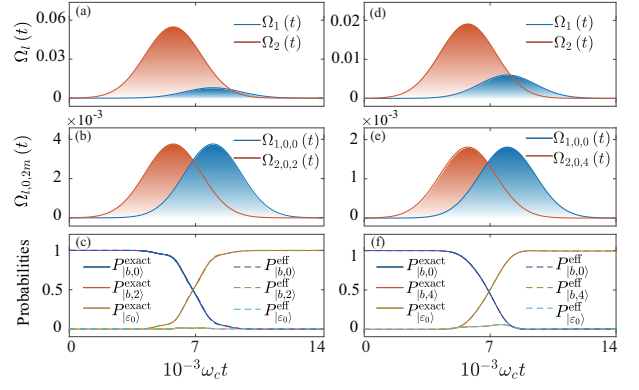


FIG. 3. (Color online) Dynamics of two- [(a)–(c)] and four-photon [(d)–(f)] generation with STIRAP. (a) and (d) The amplitudes of the Gaussian pulses in one period for two- and four-photon generation, respectively. (b) and (e) The corresponding effective coupling strengths $\Omega_{1,0,0}(t)$, $\Omega_{2,0,2}(t)$ and $\Omega_{2,0,4}(t)$ based on Eq. (9). (c) and (f) The time dependence of the probabilities of the states $|b, 2m\rangle$ ($m=0,1,2$) and $|\varepsilon_0\rangle$ under the driving pulses given in (a) and (d) respectively. The result ($P_{|j\rangle}^{\text{eff}}$) from the effective three-level system (dotted curves) agrees well with the result ($P_{|j\rangle}^{\text{exact}}$) from the exact Hamiltonian (solid curves). The parameters are (a)–(c) $\lambda/\omega_c = 0.6$, $\omega_b/\omega_c = -6$, $\Omega_1/\omega_c = 0.008$, $\Omega_2/\Omega_1 = 6.8538$, and (d)–(f) $\lambda/\omega_c = 1.2$, $\omega_b/\omega_c = -10$, $\Omega_1/\omega_c = 0.006$, $\Omega_2/\Omega_1 = 3.1814$. Other parameters are $\omega_c - \omega_g = \omega_c$, $\Delta = 0$, $\omega_c t_1 = 7960$, $\omega_c t_2 = 5760$, $\omega_c T = 2200$ and $\omega_c T_1 = 84000$.

photon generation in this process, we plot the probabilities of the states $|b, 0\rangle$, $|b, 2\rangle$, and $|\varepsilon_0\rangle$ in Fig. 3(c), from simulations of both the effective Hamiltonian and the exact Hamiltonian. Our result shows that the population in $|b, 0\rangle$ can be almost completely transferred to $|b, 2\rangle$ with its final probability reaching 1, and the probability of $|\varepsilon_0\rangle$ becomes smaller than 0.02 at the end of the STIRAP process. With the above driving parameters, the population transfer from $|b, 2\rangle$ to $|b, 4\rangle$ is negligible with the probability of $|b, 4\rangle$ on the order of 10^{-4} . This is due to the large detuning between the driving frequencies and their corresponding transition frequencies. We want to emphasize that the result [$P_{|j\rangle}^{\text{exact}}$ in Fig. 3(c)] from simulating the exact total Hamiltonian agrees well with the result [$P_{|j\rangle}^{\text{eff}}$ in Fig. 3(c)] from simulating the effective three-level Hamiltonian (14), which verifies that the three-level approximation is valid.

C. Four-photon generation

For $m = 2$ and $\Delta = 0$, the effective Hamiltonian (9) becomes

$$H_{\text{eff}}^{(4)}(t) = \Omega_{1,0,0}(t) |\varepsilon_0\rangle \langle b, 0| + \Omega_{2,0,4}(t) |\varepsilon_0\rangle \langle b, 4| + \text{H.c.}, \quad (16)$$

and the corresponding dark state (10a) has the form

$$|\psi_0^{(4)}(t)\rangle = \cos \theta_4(t) |b, 0\rangle - \sin \theta_4(t) |b, 2m\rangle, \quad (17)$$

with $\theta_4(t) = \arctan[\eta_4 \Omega_1(t) / \Omega_2(t)]$. The physical process here is similar to the process of the two-photon generation,

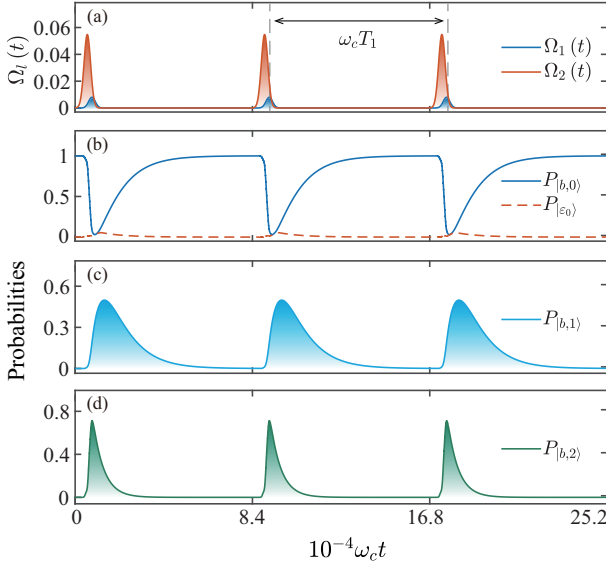


FIG. 4. (Color online) (a) The amplitude $\Omega_l(t)$ ($l=1,2$) of the Gaussian pulses as a function of the scaled time $10^{-4}\omega_c t$. (b)-(d) The probabilities $P_{|b,j\rangle}(t)$ ($j=0,1,2$) and $P_{|\epsilon_0\rangle}(t)$ vs the scaled time. The decay rates are $\kappa_a/\omega_c = \kappa_{ge}/\omega_c = \kappa_{bg}/\omega_c = 0.0001$. Other parameters are the same as those in Figs. 3(a-c).

and the efficient generation of four photons also requires an appropriate overlap between $\Omega_1(t)$ and $\Omega_2(t)$, as shown in Fig. 3(d). The corresponding effective coupling strengths $\Omega_{1,0,0}(t)$ and $\Omega_{2,0,4}(t)$ are plotted in Fig. 3(e), which also shows that the peak values of the couplings are equal to each other. The probabilities of the states $|b,0\rangle$, $|b,4\rangle$, and $|\epsilon_0\rangle$ are plotted in Fig. 3(f), which shows that the population in the state $|b,0\rangle$ can almost be completely transferred to the state $|b,4\rangle$ with the probability of $|b,4\rangle$ approaching 1, and the probability of $|\epsilon_0\rangle$ being smaller than 0.06 at the end of the STIRAP. The transfer from the state $|b,4\rangle$ to the state $|b,8\rangle$ is negligible with the probability of $|b,8\rangle$ on the order of 10^{-6} due to the large detuning in the corresponding transition. The simulation data based on the exact Hamiltonian and the effective Hamiltonian match also well in this case. This result shows that the generation of four photons can be implemented in our scheme.

IV. EMISSION OF MULTI-PHOTON BUNDLES

Photons generated in the above STIRAP process will be emitted to the cavity output via cavity dissipation. In this section, we study the multi-photon bundle emission using the following quantum master equation [12],

$$\dot{\rho}(t) = -i[H(t), \rho(t)] + \sum_{u=a,ge,bg} \sum_{n,m>n}^{\infty} \Gamma_u^{n,m} \{\mathcal{D}[|\psi_n\rangle\langle\psi_m|] \rho(t)\}, \quad (18)$$

with the superoperator $\mathcal{D}[O]\rho(t) = O\rho(t)O^\dagger - O^\dagger O\rho(t)/2 - \rho(t)O^\dagger O/2$. Here, we assume that the system-bath cou-

pling is weak with a zero-temperature Markovian bath [59], and that the total Hamiltonian $H(t)$ including the driving fields is given by Eq. (1). The state $|\psi_n\rangle$ is an eigenstate of the Hamiltonian H_0 with eigenenergy E_n , i.e., $\{|\psi_n\rangle\} = \{|b,0\rangle, |b,1\rangle, |b,2\rangle, \dots, |\epsilon_0\rangle, |\epsilon_1\rangle, \dots\}$. The relaxation rate in the superoperator $\mathcal{D}[O]$ is defined as

$$\Gamma_u^{m,n} = 2\pi d_u(\Delta_{m,n}) \alpha_u^2(\Delta_{m,n}) |C_u^{n,m}|^2, \quad (u = a, ge, bg), \quad (19)$$

which is determined by the spectral density $d_u(\Delta_{m,n})$ of the bath modes, the system-bath coupling strength $\alpha_u(\Delta_{m,n})$, and the transition matrix elements

$$\begin{aligned} C_a^{n,m} &= \langle\psi_n|(a + a^\dagger)|\psi_m\rangle, \\ C_{ge}^{n,m} &= \langle\psi_n|(|g\rangle\langle e| + |e\rangle\langle g|)|\psi_m\rangle, \\ C_{bg}^{n,m} &= \langle\psi_n|(|b\rangle\langle g| + |g\rangle\langle b|)|\psi_m\rangle. \end{aligned} \quad (20)$$

Here, $u = a$ denotes the bath for cavity damping, $u = ge, bg$ denote the baths that induce the atomic decay from $|e\rangle$ to $|g\rangle$ and from $|g\rangle$ to $|b\rangle$, respectively, and $\Delta_{m,n} = E_m - E_n$ is the transition frequency between the states $|\psi_m\rangle$ and $|\psi_n\rangle$. Note that we have neglected the Lamb-shift terms in Eq. (18). For simplicity of discussion, we assume that the spectral density $d_u(\Delta_{m,n})$ and the system-bath coupling strength $\alpha_u(\Delta_{m,n})$ be constant with the decay rate

$$\kappa_u = 2\pi d_u(\Delta_{m,n}) \alpha_u^2(\Delta_{m,n}), \quad (u = a, ge, bg). \quad (21)$$

The relaxation coefficients are then $\Gamma_u^{m,n} = \kappa_u |C_u^{n,m}|^2$.

To investigate how the cavity photons are emitted to the cavity output, we numerically calculate the probabilities $P_{|b,j\rangle}(t)$ ($j=0,1,\dots$) of the state $|b,j\rangle$ and $P_{|\epsilon_0\rangle}(t)$ of the state $|\epsilon_0\rangle$ as functions of the time t by solving Eq. (18). Furthermore, to study the statistical characteristics of the emitted photons, we numerically calculate the generalized second-order photon correlation functions of the N -photon bundle [27, 48]

$$g_N^{(2)}(t, t + \tau) = \frac{\langle X^{\dagger N}(t) X^{\dagger N}(t + \tau) X^N(t + \tau) X^N(t) \rangle}{\langle X^{\dagger N}(t) X^N(t) \rangle \langle X^{\dagger N}(t + \tau) X^N(t + \tau) \rangle}, \quad (22)$$

where the operator X is defined as

$$X = \sum_{n,m>n}^{\infty} \langle\psi_n|(a^\dagger + a)|\psi_m\rangle |\psi_n\rangle\langle\psi_m|. \quad (23)$$

Note that for $N = 1$, Eq. (22) gives the standard second-order correlation function, and at $\tau = 0$, Eq. (22) is the equal-time second-order correlation functions of N -photon bundle. In the following, we will focus on two- and four-photon bundle emission to illustrate our approach. We want to note that higher numbers of photons can be generated with this scheme. For example, six-photon bundle can be created when the virtual-photon coefficient $C_{0,6}$ becomes significant in the deep-strong coupling regime with $\lambda/\omega_c > 1$, as shown in Fig. 2. The deep-strong coupling regime has already been realized in superconducting circuits with $(\lambda/\omega_c = 1.34)$ [7] and in Landau-polariton systems with $(\lambda/\omega_c = 1.43)$ [8].

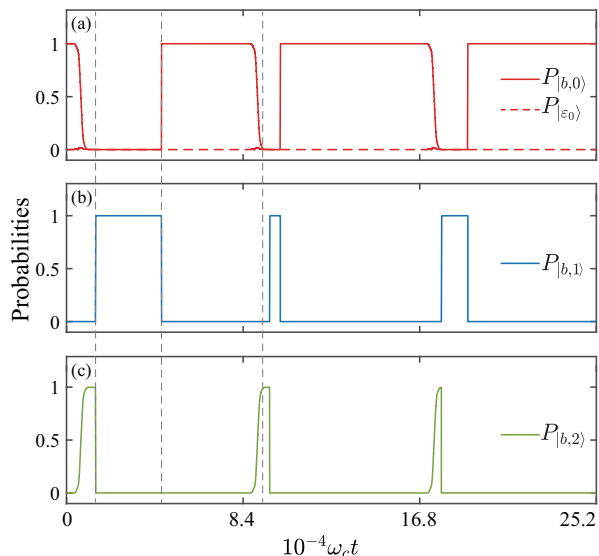


FIG. 5. (Color online) Quantum trajectories of the probabilities of the states $|b, j\rangle$ ($j = 0, 1, 2$) and $|\varepsilon_0\rangle$ in the two-photon bundle emission. The parameters are the same as those in Fig. 4.

A. Two-photon bundle

We first consider the emission of two-photon bundles from the dissipative cavity. In Fig. 4(a), the Gaussian pulses of the two driving fields are presented over three cycles of the STIRAP process. The cycles are separated by the duration T_1 . In Figs. 4(b-d), we plot the probabilities $P_{|b,0\rangle}$, $P_{|b,1\rangle}$, $P_{|b,2\rangle}$, and $P_{|\varepsilon_0\rangle}$ as functions of the normalized time $10^{-4}\omega_c t$. After applying the Gaussian pulse $\Omega_2(t)$ followed by the Gaussian pulse $\Omega_1(t)$, as shown in Fig. 4(a), we find that the initial state $|b, 0\rangle$ is effectively transferred to $|b, 2\rangle$ with a probability 0.713 under the parameters $\lambda/\omega_c = 0.6$, $\omega_b/\omega_c = -6$, $\Omega_1/\omega_c = 0.008$, $\Omega_2/\Omega_1 = 6.8538$, and $\kappa_u/\omega_c = 0.0001$ ($u = a, ge, bg$). Because of finite cavity dissipation during the STIRAP, the state conversion probability is smaller than 1. The generated photons are then emitted to the cavity output by the decay processes $|b, 2\rangle \rightarrow |b, 1\rangle \rightarrow |b, 0\rangle$, and the system returns to the initial state $|b, 0\rangle$ after the emissions. The emission cycle repeats itself after a duration T_1 , which needs to be sufficiently long to ensure the system returns to the initial state $|b, 0\rangle$ before the start of the next emission cycle. Here the Gaussian pulses $\Omega_l(t)$ ($l = 1, 2$) satisfy the condition (13) in order to achieve effective generation of the photon bundle.

To study the dynamical emission of the photons, we simulate an initial quantum system by using the quantum jump approach [60, 61]. In Figs. 5(a-c), we plot the quantum trajectory of the probabilities of the states $|b, j\rangle$ ($j=0,1,2$) and $|\varepsilon_0\rangle$ starting from the initial state $|b, 0\rangle$. Our result shows that after the STIRAP, the population in the state $|b, 2\rangle$ is almost one as can be seen in Fig. 5(c). After the first photon is emitted out of the cavity, the system state collapses to $|b, 1\rangle$ with a probability almost equal to 1, as shown in Fig. 5(b). After the second photon is emitted, the system returns to the initial state $|b, 0\rangle$ as shown in Fig. 5(a). This result hence illustrates the two-

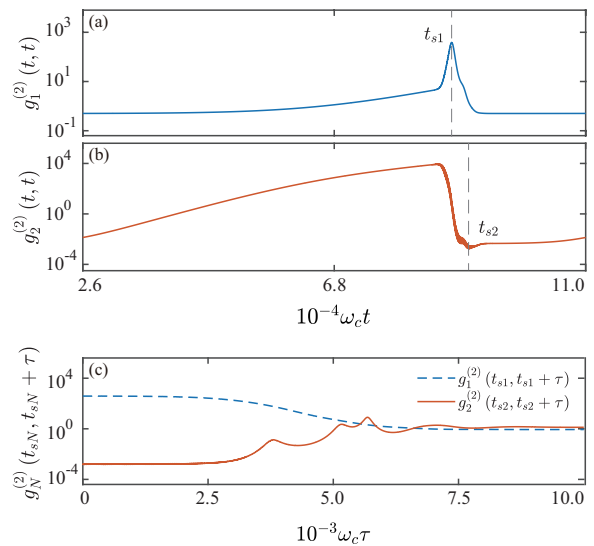


FIG. 6. (Color online) The equal-time and time-delayed second-order correlation functions for two-photon emission. (a) $g_1^{(2)}(t, t)$ and (b) $g_2^{(2)}(t, t)$ vs time t . The t_{s1} (t_{s2}) is the time corresponding to the maximum (minimum) value of $g_1^{(2)}(t, t)$ [$g_2^{(2)}(t, t)$]. (c) $g_N^{(2)}(t_{sN}, t_{sN} + \tau)$ for $N=1$ and $N=2$ vs the time delay τ . The parameters are the same as those in Fig. 4.

photon bundle emission where the two photons are separated by a short temporal window determined by the cavity decay rate.

To investigate the statistical properties of the emitted photons, we numerically calculate the standard and generalized equal-time second-order correlation functions for $N=1$ and $N=2$ given by Eq. (22) at $\tau = 0$. In Fig. 6(a), we plot the standard equal-time second-order correlation function $g_1^{(2)}(t, t)$ within one emission cycle. We find that the maximum value of $g_1^{(2)}(t, t)$ at the time t_{s1} is larger than one. This result implies that the photons are in a super-Poisson distribution with more than one photons emitted in the system. In Fig. 6(b), we plot the generalized equal-time second-order correlation function $g_2^{(2)}(t, t)$ within one emission cycle. The minimum value of $g_2^{(2)}(t, t)$ at the time t_{s2} is smaller than one, which corresponds to a sub-Poisson distribution of the emitted photon bundles. We also calculate the time-delayed second-order correlation functions $g_1^{(2)}(t_{s1}, t_{s1} + \tau)$ and $g_2^{(2)}(t_{s2}, t_{s2} + \tau)$ as defined in Eq. (22). Our result is given in Fig. 6(c). It can be seen that $g_1^{(2)}(t_{s1}, t_{s1}) > g_1^{(2)}(t_{s1}, t_{s1} + \tau)$ and $g_2^{(2)}(t_{s2}, t_{s2}) < g_2^{(2)}(t_{s2}, t_{s2} + \tau)$. This result further confirms that the emitted photons are bunched while the two-photon bundles are antibunched. Hence our scheme can lead to the construction of a two-photon antibunched emitter.

B. Four-photon bundle

Next we study the generation of four-photon bundle by using STIRAP. In Fig. 7(a), the external Gaussian pulses $\Omega_1(t)$ and $\Omega_2(t)$ are given, which satisfy the condition (13). Similar

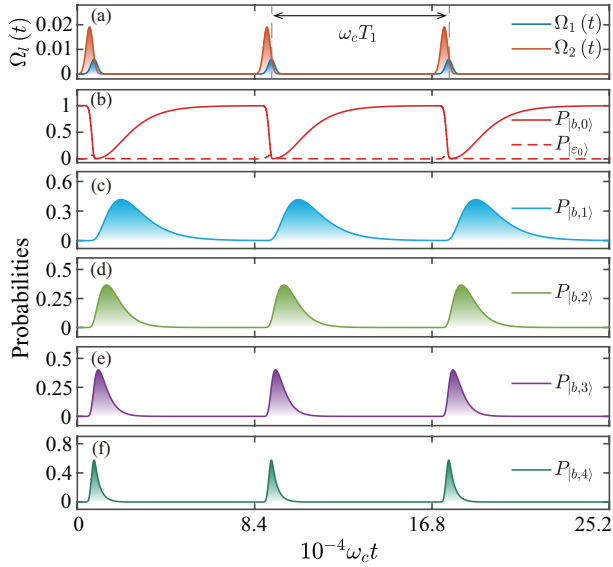


FIG. 7. (Color online) (a) The amplitude $\Omega_l(t)$ ($l=1,2$) of the Gaussian pulses as a function of the scaled time $10^{-4}\omega_c t$. (b)-(f) The probabilities $P_{|b,j\rangle}(t)$ ($j=0,1,2,3,4$) and $P_{|\varepsilon_0\rangle}(t)$ vs the scaled time. The decay rates are $\kappa_a/\omega_c = \kappa_{ge}/\omega_c = \kappa_{bg}/\omega_c = 0.0001$. Other parameters are the same as those in Figs. 3(d-f).

to the studies for two-photon bundle, we calculate the probabilities $P_{|b,j\rangle}(t)$ on the state $|b, j\rangle$ ($j=0,1,2,3,4$) and $P_{|\varepsilon_0\rangle}(t)$ on the state $|\varepsilon_0\rangle$, which are plotted in Figs. 7(b-f). It can be shown that after the applied Gaussian pulses, the initial state $|b, 0\rangle$ is effectively transferred to the four-photon state $|b, 4\rangle$ with a probability 0.575. The parameters used here are $\lambda/\omega_c = 1.2$, $\omega_b/\omega_c = -10$, $\Omega_1/\omega_c = 0.006$, $\Omega_2/\Omega_1 = 3.1814$, and $\kappa_u/\omega_c = 0.0001$ ($u = a, ge, bg$). The cavity dissipation during the external pulses reduces the efficiency of the population transfer to be less than one. The generated photons will then decay to the cavity output one by one with $|b, 4\rangle \rightarrow |b, 3\rangle \rightarrow |b, 2\rangle \rightarrow |b, 1\rangle \rightarrow |b, 0\rangle$, and the system will return to the initial state $|b, 0\rangle$ after all photons are emitted. The cycle will repeat when the next set of Gaussian pulses are applied. We want to point out that the time interval T_1 of the cycles satisfies the condition: $\kappa_a T_1 \gg 1$, so that our photons will be released outside the cavity when the next cycle begins.

We use the quantum jump approach to obtain the quantum trajectory in this four-photon generation process. One quantum trajectory of the probabilities $P_{|b,j\rangle}(t)$ ($j=0,1,2,3,4$) and $P_{|\varepsilon_0\rangle}(t)$ is presented in Figs. 8(a-e). It can be seen that four photons appear in the cavity after the applied Gaussian pulses, then the photons are emitted to the cavity output one by one with a short temporal window between adjacent output photons with the final state returning to the initial state $|b, 0\rangle$. The result shows that the four photons are emitted in a bundle before the next cycle begins.

To understand the statistical properties of the generated photons, we calculate the equal-time second-order correlation functions for single photon $g_1^{(2)}(t, t)$ and four photons $g_4^{(2)}(t, t)$, respectively, as given in Figs. 9(a, b). We find that the maximum value of $g_1^{(2)}(t, t)$ at the time t_{s1} is larger than one, which

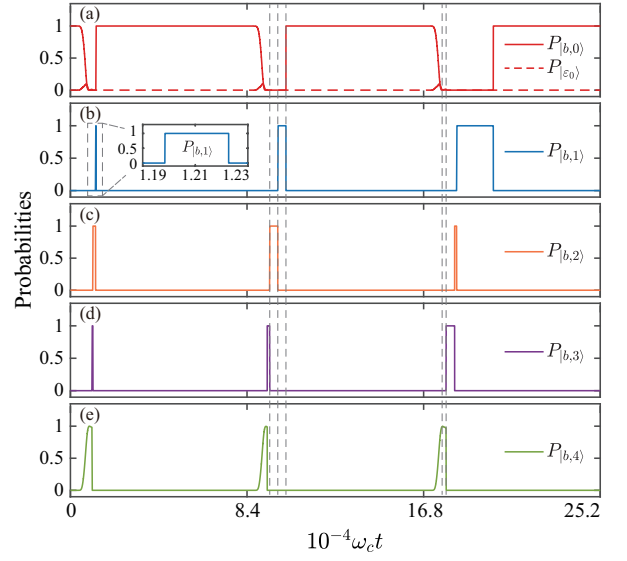


FIG. 8. (Color online) Quantum trajectories of the probabilities of the states $|b, j\rangle$ ($j = 0, 1, 2, 3, 4$) and $|\varepsilon_0\rangle$ in the four-photon bundle emission. The parameters are the same as those in Fig. 7.

shows that the generated photons are in a super-Poisson distribution at t_{s1} . Meanwhile, the minimum value of $g_4^{(2)}(t, t)$ at the time t_{s4} is smaller than one, which indicates that the four-photon bundles are in a sub-Poisson distribution at t_{s4} . To characterize the statistics of the emitted four-photon bundle, we further study the time-delayed second-order correlation functions $g_1^{(2)}(t_{s1}, t_{s1} + \tau)$ and $g_4^{(2)}(t_{s4}, t_{s4} + \tau)$ following the definition in Eq. (22). The numerical result of the time-delayed correlation functions is given in Fig. 9(c). Similar to that of the two-photon bundle, $g_1^{(2)}(t_{s1}, t_{s1}) > g_1^{(2)}(t_{s1}, t_{s1} + \tau)$, indicates bunched single-photon behavior, and $g_4^{(2)}(t_{s4}, t_{s4}) < g_4^{(2)}(t_{s4}, t_{s4} + \tau)$, indicates antibunched behavior for the four-photon bundles. This result verifies that the scheme gives a method to implement an antibunched four-photon bundle emitter.

V. CONCLUSION AND DISCUSSION

We proposed a deterministic approach to generate multi-photon bundles via virtual-photon STIRAP for a Ξ -type atom coupled to a cavity mode in the ultrastrong or deep-strong coupling regime. By applying two appropriately designed Gaussian pulses, the system state can be transferred on-demand to a multi-photon state via the STIRAP technique. The photons will then decay to the cavity output in a bundle. By studying the quantum trajectory of the system and the standard and generalized second-order correlation functions, we find that the emitted single photons are in a super-Poisson distribution and the emitted multi-photon bundles are antibunched in a sub-Poisson distribution. This scheme provides a venue to implement efficient, on-demand multi-photon emitters.

In this work, we only discussed the generation of even numbers of photons based on the selection of the driving param-

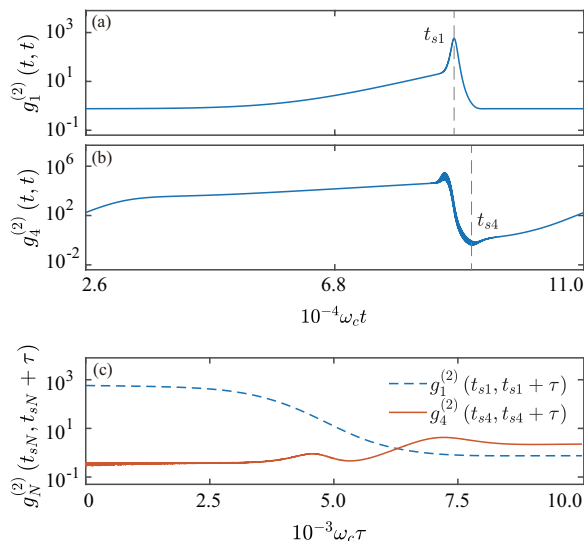


FIG. 9. (Color online) The equal-time and time-delayed second-order correlation functions for four-photon emission. (a) $g_1^{(2)}(t, t)$ and (b) $g_4^{(2)}(t, t)$ vs time t . The t_{s1} (t_{s4}) is the time corresponding to the maximum (minimum) value of $g_1^{(2)}(t, t)$ [$g_4^{(2)}(t, t)$]. (c) $g_N^{(2)}(t_{sN}, t_{sN} + \tau)$ for $N=1$ and $N=4$ vs the time delay τ . The parameters are the same as those in Fig. 7.

eters in the calculation. We want to point out odd numbers of photon bundle emitters can also be created. By adjusting the frequencies of the driving pulses to aim at the first excited state $|\varepsilon_1\rangle$ of the QRM, on-demand single photon emitter or tri-photon emitter can be realized. Note that the successful generation of desired multi-photon bundles requires that the duration of the pulse cycle T_1 is sufficiently long with $\kappa_a T_1 \gg 1$, so that the system can return to the proper initial state $|b, 0\rangle$ before the next cycle starts.

The realization of our scheme is within reach of current state-of-the-art experimental technology. The ultrastrong and deep-strong coupling regimes have been realized in several platforms, such as superconducting circuits [1, 2, 7, 9], intersubband polaritons [5], Landau polaritons [8, 10], organic molecules [3, 6], and optomechanics [4]. Hence our method is a practical approach that can lead to the construction of on-demand multi-photon sources.

ACKNOWLEDGMENTS

J.-F.H. is supported in part by the National Natural Science Foundation of China (Grant No. 12075083), and Natural Science Foundation of Hunan Province, China (Grant No. 2020JJ5345). L.T. is supported by the National Science Foundation (Awards No. 2006076 and No. 2037987).

-
- [1] T. Niemczyk, F. Deppe, H. Huebl, E. P. Menzel, F. Hocke, M. J. Schwarz, J. J. García-Ripoll, D. Zueco, T. Hümmer, E. Solano, A. Marx, and R. Gross, *Nat. Phys.* **6**, 772 (2010).
- [2] P. Forn-Díaz, J. Lisenfeld, D. Marcos, J. J. García-Ripoll, E. Solano, C. J. P. M. Harmans, and J. E. Mooij, *Phys. Rev. Lett.* **105**, 237001 (2010).
- [3] T. Schwartz, J. A. Hutchison, C. Genet, and T. W. Ebbesen, *Phys. Rev. Lett.* **106**, 196405 (2011).
- [4] F. Benz, M. K. Schmidt, A. Dreismann, R. Chikkaraddy, Y. Zhang, A. Demetriadou, C. Carnegie, H. Ohadi, B. de Nijs, R. Esteban, J. Aizpurua, and J. J. Baumberg, *Science* **354**, 726 (2016).
- [5] B. Askenazi, A. Vasanelli, Y. Todorov, E. Sakat, J.-J. Greffet, G. Beaudoin, I. Sagnes, and C. Sirtori, *ACS photonics* **4**, 2550 (2017).
- [6] F. Barachati, J. Simon, Y. A. Getmanenko, S. Barlow, S. R. Marder, and S. Kéna-Cohen, *ACS Photonics* **5**, 119 (2018).
- [7] F. Yoshihara, T. Fuse, S. Ashhab, K. Kakuyanagi, S. Saito, and K. Semba, *Nat. Phys.* **13**, 44 (2017).
- [8] A. Bayer, M. Pozimski, S. Schambeck, D. Schuh, R. Huber, D. Bougeard, and C. Lange, *Nano Lett.* **17**, 6340 (2017).
- [9] F. Yoshihara, T. Fuse, Z. Ao, S. Ashhab, K. Kakuyanagi, S. Saito, T. Aoki, K. Koshino, and K. Semba, *Phys. Rev. Lett.* **120**, 183601 (2018).
- [10] V. M. Muravev, I. V. Andreev, I. V. Kukushkin, S. Schmult, and W. Dietsche, *Phys. Rev. B* **83**, 075309 (2011).
- [11] P. Nataf and C. Ciuti, *Phys. Rev. Lett.* **104**, 023601 (2010).
- [12] A. Ridolfo, M. Leib, S. Savasta, and M. J. Hartmann, *Phys. Rev. Lett.* **109**, 193602 (2012).
- [13] Z. H. Wang, Y. Li, D. L. Zhou, C. P. Sun, and P. Zhang, *Phys. Rev. A* **86**, 023824 (2012).
- [14] T. Shi, Y. Chang, and J. J. García-Ripoll, *Phys. Rev. Lett.* **120**, 153602 (2018).
- [15] M.-J. Hwang, R. Puebla, and M. B. Plenio, *Phys. Rev. Lett.* **115**, 180404 (2015).
- [16] X. Chen, Z. Wu, M. Jiang, X.-Y. Lü, X. Peng, and J. Du, *Nat. Commun.* **12**, 6281 (2021).
- [17] M.-L. Cai, Z.-D. Liu, W.-D. Zhao, Y.-K. Wu, Q.-X. Mei, Y. Jiang, L. He, X. Zhang, Z.-C. Zhou, and L.-M. Duan, *Nat. Commun.* **12**, 1126 (2021).
- [18] L. Garziano, R. Stassi, V. Macrì, A. F. Kockum, S. Savasta, and F. Nori, *Phys. Rev. A* **92**, 063830 (2015).
- [19] K. K. W. Ma, *Phys. Rev. A* **102**, 053709 (2020).
- [20] J.-F. Huang and C. K. Law, *Phys. Rev. A* **91**, 023806 (2015).
- [21] J.-F. Huang, J.-Q. Liao, L. Tian, and L.-M. Kuang, *Phys. Rev. A* **96**, 043849 (2017).
- [22] J.-F. Huang, J.-Q. Liao, and L.-M. Kuang, *Phys. Rev. A* **101**, 043835 (2020).
- [23] J.-F. Huang and L. Tian, arXiv:2208.12524.
- [24] R. Stassi, A. Ridolfo, O. Di Stefano, M. J. Hartmann, and S. Savasta, *Phys. Rev. Lett.* **110**, 243601 (2013).
- [25] J.-F. Huang and C. K. Law, *Phys. Rev. A* **89**, 033827 (2014).
- [26] M. Cirio, S. De Liberato, N. Lambert, and F. Nori, *Phys. Rev. Lett.* **116**, 113601 (2016).
- [27] C. S. Muñoz, E. del Valle, A. G. Tudela, K. Müller, S. Lichtmannecker, M. Kaniber, C. Tejedor, J. J. Finley, and F. P. Laussy, *Nat. Photonics* **8**, 550 (2014).
- [28] H. Walther, B. T. H. Varcoe, B.-G. Englert, and T. Becker, *Rep. Prog. Phys.* **69**, 1325 (2006).
- [29] J. L. O'Brien, A. Furusawa, and J. Vučković, *Nat. Photonics* **3**, 687 (2009).
- [30] V. Giovannetti, S. Lloyd, and L. Maccone, *Science* **306**, 1330

- (2004).
- [31] V. Giovannetti, S. Lloyd, and L. Maccone, *Phys. Rev. Lett.* **96**, 010401 (2006).
- [32] M. D'Angelo, M. V. Chekhova, and Y. Shih, *Phys. Rev. Lett.* **87**, 013602 (2001).
- [33] H. J. Kimble, *Nature (London)* **453**, 1023 (2008).
- [34] P. Ball, *Nature (London)* **474**, 272 (2011).
- [35] N. Sim, M. F. Cheng, D. Bessarab, C. M. Jones, and L. A. Krivitsky, *Phys. Rev. Lett.* **109**, 113601 (2012).
- [36] W. Denk, J. H. Strickler, and W. W. Webb, *Science* **248**, 73 (1990).
- [37] N. G. Horton, K. Wang, D. Kobat, C. G. Clark, F. W. Wise, C. B. Schaffer, and C. Xu, *Nat. Photonics* **7**, 205 (2013).
- [38] P. Bienias, S. Choi, O. Firstenberg, M. F. Maghrebi, M. Gullans, M. D. Lukin, A. V. Gorshkov, and H. P. Büchler, *Phys. Rev. A* **90**, 053804 (2014).
- [39] M. F. Maghrebi, M. J. Gullans, P. Bienias, S. Choi, I. Martin, O. Firstenberg, M. D. Lukin, H. P. Büchler, and A. V. Gorshkov, *Phys. Rev. Lett.* **115**, 123601 (2015).
- [40] J.-Q. Liao and C. K. Law, *Phys. Rev. A* **82**, 053836 (2010).
- [41] A. Miranowicz, M. Paprzycka, Y.-x. Liu, J. c. v. Bajer, and F. Nori, *Phys. Rev. A* **87**, 023809 (2013).
- [42] A. Dousse, J. Suffczyński, A. Beveratos, O. Krebs, A. Lemaître, I. Sagnes, J. Bloch, P. Voisin, and P. Senellart, *Nature (London)* **466**, 217 (2010).
- [43] Y. Ota, S. Iwamoto, N. Kumagai, and Y. Arakawa, *Phys. Rev. Lett.* **107**, 233602 (2011).
- [44] M. Müller, S. Bounouar, K. D. Jöns, M. Glässl, and P. Michler, *Nat. Photonics* **8**, 224 (2014).
- [45] Y. Chang, A. González-Tudela, C. Sánchez Muñoz, C. Navarrete-Benlloch, and T. Shi, *Phys. Rev. Lett.* **117**, 203602 (2016).
- [46] D. V. Strekalov, *Nat. Photonics* **8**, 500 (2014).
- [47] C. S. M. noz, F. P. Laussy, E. del Valle, C. Tejedor, and A. González-Tudela, *Optica* **5**, 14 (2018).
- [48] Q. Bin, Y. Wu, and X.-Y. Lü, *Phys. Rev. Lett.* **127**, 073602 (2021).
- [49] Y. G. Deng, T. Shi, and S. Yi, *Photonics Res.* **9**, 1289 (2021).
- [50] S.-I. Ma, X.-k. Li, Y.-I. Ren, J.-k. Xie, and F.-I. Li, *Phys. Rev. Research* **3**, 043020 (2021).
- [51] A. González-Tudela, V. Paulisch, D. E. Chang, H. J. Kimble, and J. I. Cirac, *Phys. Rev. Lett.* **115**, 163603 (2015).
- [52] J. S. Douglas, T. Caneva, and D. E. Chang, *Phys. Rev. X* **6**, 031017 (2016).
- [53] A. González-Tudela, V. Paulisch, H. J. Kimble, and J. I. Cirac, *Phys. Rev. Lett.* **118**, 213601 (2017).
- [54] K. Bergmann, H. Theuer, and B. W. Shore, *Rev. Mod. Phys.* **70**, 1003 (1998).
- [55] N. V. Vitanov, A. A. Rangelov, B. W. Shore, and K. Bergmann, *Rev. Mod. Phys.* **89**, 015006 (2017).
- [56] Y.-H. Liu, X.-L. Yin, J.-F. Huang, and J.-Q. Liao, *Phys. Rev. A* **105**, 023504 (2022).
- [57] I. I. Rabi, *Phys. Rev.* **49**, 324 (1936).
- [58] D. Braak, *Phys. Rev. Lett.* **107**, 100401 (2011).
- [59] H.-P. Breuer and F. Petruccione, *The theory of open quantum systems* (Oxford University Press on Demand, 2002).
- [60] M. B. Plenio and P. L. Knight, *Rev. Mod. Phys.* **70**, 101 (1998).
- [61] A. J. Daley, *Adv. Phys.* **63**, 77 (2014).